LARGE AREA SOLAR CELLS WITH SCREEN PRINTED FRONT SIDE METALLIZATION AND DIELECTRIC REAR SIDE PASSIVATION

Regina Pavlović, Amir Dastgheib-Shirazi, Felix Book, Bernd Raabe, Giso Hahn
University of Konstanz, Department of Physics; P.O. Box X916, 78457 Konstanz, Germany
Phone: +49 7531 883731, fax: +49 7531 883895, e-mail: regina.pavlovic@uni-konstanz.de

ABSTRACT: In this work we investigated local rear contact structures and compared these to the full area Al-BSF structure. Two processes for local contacts are presented: The laser fired contact (LFC) process and a screen printing process to create a local back surface field (SP-LBSF) structure. The rear side passivation is provided by a firing stable SiO_2/SiN_x-stack, using a thin dry thermal SiO_2 and a PECVD SiN_x. We analyzed several process schemes to implement the local rear side structure with a screen printed front side metallization. As a flat rear side is very important for a successful implementation of a solar cell process with dielectric layer passivation, we focused on these processes. Monocrystalline Cz-Si solar cells (cell size 125x125 mm²) with an LFC structure and up to 17.6% efficiency were processed. The fabricated LFC cells show an increased reflectivity at long wavelengths due to the evaporated aluminum on the rear side. Furthermore, the internal quantum efficiency of the LFC and the SP-LBSF solar cells in the long wavelength range is significantly higher than for solar cells with aluminum back surface field.
Keywords: Metallization, Manufacturing and Processing, Laser Processing

1 INTRODUCTION

Although local rear contact structures are under investigation since several years, they are still not implemented in the production of industrial-type large area solar cells. Excellent results were achieved for small area solar cells using high efficiency processes [1]. In this work we processed large area solar cells with screen printed front side metallization, dielectric rear side passivation and local rear side contacts using Czochralski (Cz) silicon material. Two local rear contact structures are studied and compared to the screen printed full area Al-BSF structure: The LFC [2] and the SP-LBSF structure are shown schematically in Fig. 1. For the LFC structure, several manufacturing processes were investigated. The SP-LBSF structure was realized by a screen printing process [3].
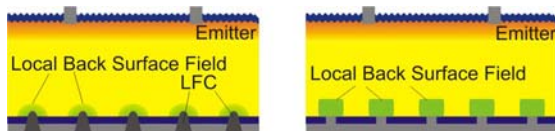
Figure 1: Schemes of the investigated local rear contact structures. LFC concept (left) and SP-LBSF concept (right).

2 PROCESSING SEQUENCES

2.1 LFC process

In this work a processing sequence for solar cells with LFC rear side was developed. The first processing sequence included a textured rear side. The passivation quality of a textured surface is lower compared to a flat surface with the same passivation layer [4]. Thus the processing sequence was extended by steps to etch the rear side texture. Due to the many etching steps, the wafers tend to get very thin. As an alternative to reduce the silicon loss, the rear side was processed and masked before texturization in the next process under investigation. This processing sequence is displayed in Fig. 2 (left). For rear side processing, the wafers were

saw damage etched and cleaned. Then a 20 nm thick thermal SiO_2 layer and a 120 nm plasma enhanced chemical vapor deposition (PECVD) SiN_x layer were deposited as dielectric rear side passivation. After etching the oxide on the front side, the wafers were textured and the emitter diffusion was done in a $POCl_3$ tube furnace. A PECVD SiN_x layer was deposited as anti reflection coating and the front side was metallized by screen printing silver paste and firing was done in a belt furnace. The firing parameters were optimized by measuring the contact resistance with the transmission line method (TLM). We chose the lowest temperature that led to a sufficiently low contact resistance between the contact finger structure and the emitter. After evaporating the aluminum on the rear side, the laser fired contacts were applied and the edge isolation was also performed with the laser. At last the solar cells were sintered in a hydrogen atmosphere in the microwave induced remote hydrogen plasma (MIRHP) reactor to improve the contact and the surface passivation on the rear side.

Figure 2: Processing sequences of the investigated solar cell concepts. The processing steps needed for the screen printed Al-BSF concept are marked green, whereas the ones for the LFC or SP-LBSF concept are yellow or orange.

2.2 SP-LBSF process

In the SP-LBSF concept, aluminum paste is screen printed on the rear side. Screen printing aluminum on the rear is widely used in industry, in contrast to aluminum evaporation in the above mentioned LFC process. The processing sequence was based on the sequence developed for the LFC process and is displayed in Fig. 2 (right). Only the metallization steps differ from the ones in the LFC process. In order to contact the rear side, the dielectric passivation layer was etched locally by an etching paste. The etching paste was screen printed onto the wafer. The wafer was then heated for approximately one minute on a hot plate at approximately 400 °C. The paste residues were removed in an ultrasonic bath. After sintering the wafers in the MIRHP reactor to improve the rear surface passivation, front and rear contacts were screen printed and fired. At last the edges were isolated by a laser.

3   CONTACT DISTANCE

An increased contact distance at the rear leads to a reduced contact area which may cause series resistance problems, but also to a larger dielectrically passivated area. Therefore, the contact distance for the LFC contacts was optimized and the influence of the contact distance on contact resistance and carrier lifetime was investigated.

3.1 Contact resistance

To investigate the influence of the contact distance on contact resistance, symmetrical samples (4 cm^2) were processed. We used 1-3 Ωcm boron doped Cz-Si material which is comparable to the material the solar cells were fabricated from. The wafers were passivated with a 20 nm thermal oxide and some had an additional 75 nm PECVD SiN_x layer on both sides. Aluminum was evaporated on both sides and the samples were contacted with the laser. As expected, the contact resistance decreases with increasing contact area, the results of the measurements are displayed in Fig. 3.
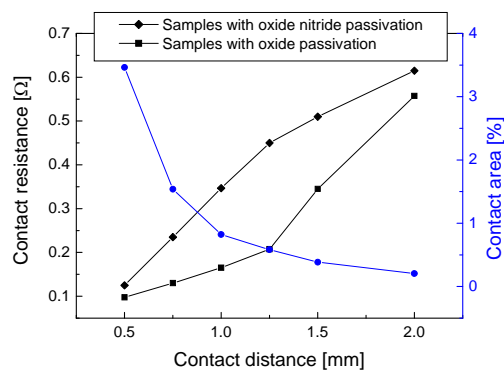
Figure 3: Contact resistance and area versus the contact distance.

3.2 Carrier lifetime

To ascertain the optimal contact distance, symmetrical $5 \times 5 \text{ cm}^2$ FZ carrier lifetime samples with $R_{base} = 0.5 \ \Omega$cm were processed. They were passivated on both sides with a 20 nm thick thermal SiO_2 and 120 nm

thick PECVD SiN_x. Then the aluminum was evaporated and the samples were contacted with different contact distances from 0.5 mm to 1.5 mm using a laser. Subsequently the aluminum was etched off with HCl and the effective lifetime was measured by quasi steady state photoconductance (QSSPC) and microwave-induced photoconductivity decay (MW-PCD). There was no significant difference in carrier lifetime measured for the samples with 0.5 mm, 0.8 mm, 1.0 mm and 1.2 mm contact distance. Only the samples with a contact distance of 1.5 mm had a significant higher carrier lifetime. Thus the contact distance can be varied in the range of 0.5 mm to 1.2 mm with a negligible effect on the effective carrier lifetime.

3.3 LFC solar cells with different contact distances

As the optimal contact distance could not be determined by carrier lifetime and contact resistance samples we processed solar cells with different contact distances.

The solar cells were processed as displayed in Fig. 2. We used Cz-Si material with 2-5 Ωcm and 240 μm thickness and chose distances of 0.4 mm, 0.8 mm and 1.6 mm. Additionally, references with a full area screen printed Al-BSF were processed. The IQE shows a better performance at long wavelengths for higher contact distances (see Fig. 4). Comparing the solar cell results, one can see a decreasing fill factor and increasing short circuit current and open circuit voltage for increasing contact distance. The efficiency is therefore highest at the medium distance of 0.8 mm (see Table I and Fig. 8), as the effects point in opposite directions.
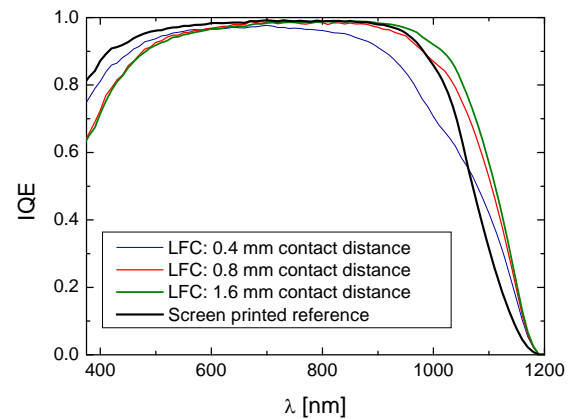
Figure 4: IQE of LFC solar cells with different contact distances and a screen printed reference.

Table I: Average solar cell results of solar cells with different contact distances.

| Contact distance [mm]	FF [%]	J_{SC} [mA/cm^2]	V_{OC} [mV]	η [%]
0.4	77.5	34.3	613	16.3
0.8	76.8	35.2	624	16.9
1.6	62.8	36.0	630	14.2

4 MIRHP PROCESS

4.1 Contact resistance

A reduced contact resistance was measured with the symmetrical carrier lifetime samples as described above after sintering in the MIRHP in a hydrogen atmosphere at approximately 380 °C for 30 min. The average contact resistance before sintering was 0.31 Ω, afterwards the contact resistance could be reduced to 0.18 Ω.

4.2 Passivation

The enhanced passivation quality after the MIRHP step can be seen in the IQE of a solar cell (Fig. 5). The IQE of the solar cell at long wavelengths is higher after passivation.
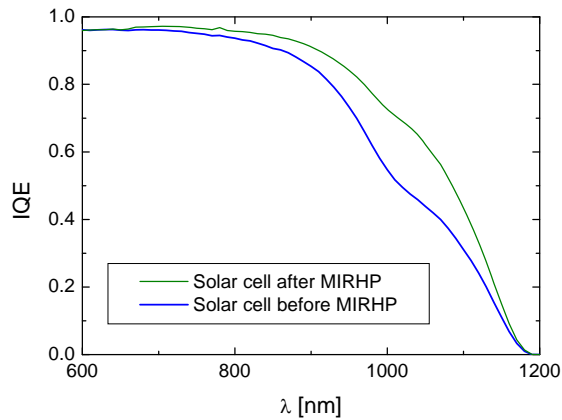
Figure 5: IQE of a solar cell before and after MIRHP processing.

5 CONTACT PROPERTIES

5.1 Proportions of laser fired contacts

In Fig. 6 microscope pictures of laser fired contacts are shown. On the left picture one can see the LFC after laser firing, on the right the aluminum was removed by etching. The aluminum could not be etched by HCl in the center of the LFC. In this area the aluminum and the silicon probably formed an eutectic. At the border of the remaining aluminum the color gradient of the silicon nitride layer is visible. In both LFC pictures there is an inner and outer region of the LFC. The diameter of the inner region is in both cases approximately 90 µm. Presumably the contacts are formed in this area.
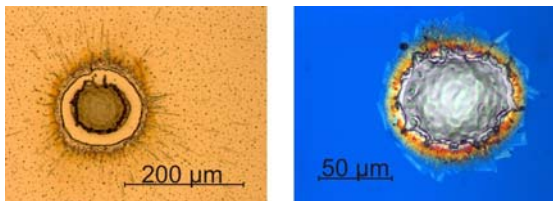
Figure 6: Microscope pictures of an LFC after laser firing (left) and after etching of the aluminum (right).

5.2 Proportions of local screen printed contacts

The proportions of the screen for the etching of the silicon nitride layer were based on the ones of the laser fired contacts. The screen had quadratic openings with an edge length of 100 µm. Fig. 7 shows a microscope picture of an etched contact area and the profile of a complete contact. The diameter of a local screen printed contact is approximately 120 µm.
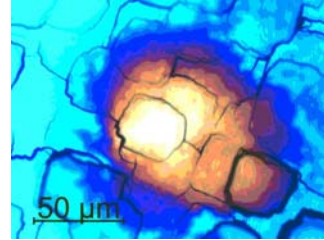
Figure 7: Microscope picture of a contact area etched with screen printed etching paste.

6 COMPARISON OF DIFFERENT REAR SIDE STRUCTURES

6.1 Solar cell results

LFC solar cells with up to 17.6% efficiency were processed on Cz-Si material. The results are displayed in Table II. The performance of the LFC solar cell is similar to that of the solar cell with full area Al-BSF.

Solar cells with local screen printed contacts and LFC cells of the same batch are shown in Table III. The contact distance of the SP-LBSF solar cells was not optimized separately. We chose also a distance of 0.8 mm based on the result of the LFC solar cells. The resulting efficiency values are very similar. The open circuit voltage of the SP-LBSF cells is decreased compared to the LFC cells. Due to the flat front side, the short circuit current is lower than in the batch displayed in Table II. Additionally, the metal grid on the front side is wider compared to the other batch, because of the flat front side. This led to increased shadowing which reduced the values for the open circuit voltage further (Fig. 8).

Table II: Solar cell results of the best solar cells with LFC and full area Al-BSF rear side (textured front side).

Cell	FF [%]	J_{SC} [mA/cm^2]	V_{OC} [mV]	η [%]
LFC	78.0	35.7	633	17.6
Al-BSF	79.2	35.4	632	17.7

Table III: Solar cell results of the best LFC cell and SP-LBSF cell of one batch (untextured front side).

| Cell	FF [%]	J_{SC} [mA/cm^2]	V_{OC} [mV]	η [%]
SP-LBSF	78.9	31.5	621	15.4
LFC	76.7	31.8	626	15.3
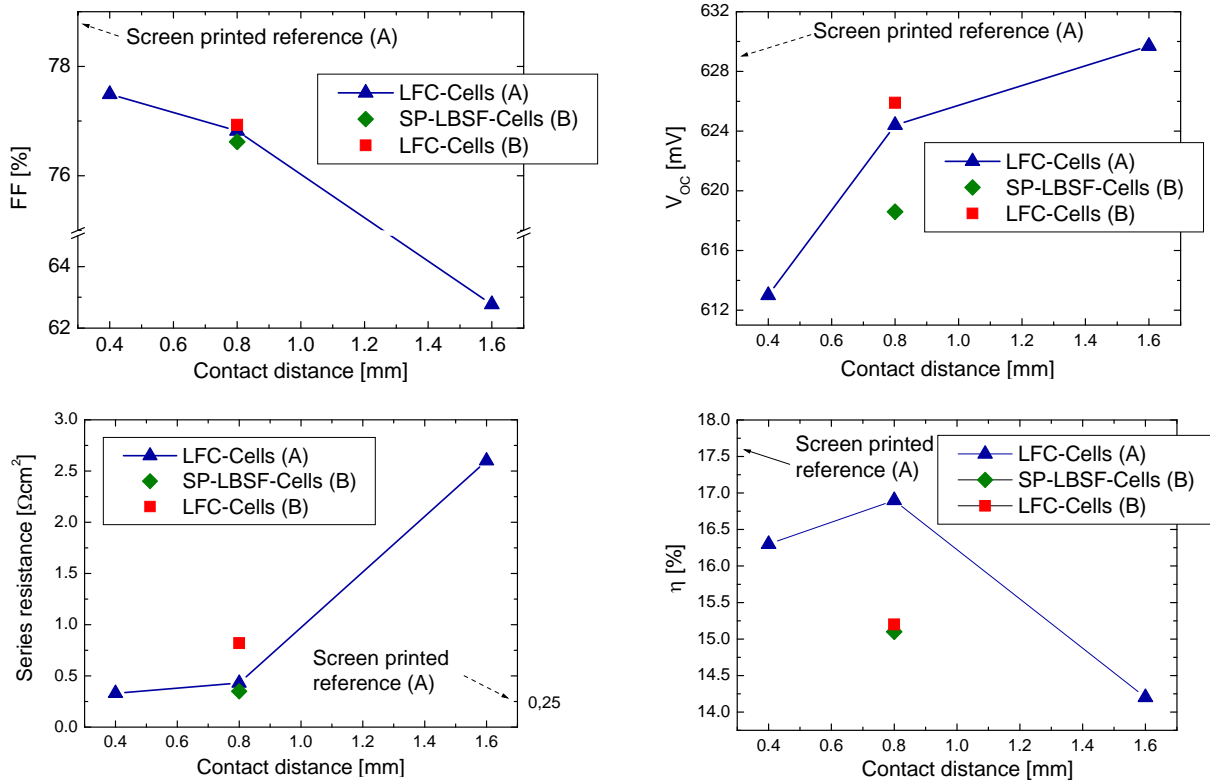
Figure 8: Average values of FF, V_{OC}, the fitted series resistance and efficiency for the different solar cell concepts. The solar cells were processed in two different batches, A (textured front side) and B (untextured front side).

6.2 Internal quantum efficiency and reflection

An improvement in the internal quantum efficiency at long wavelengths could be seen on both locally contacted solar cell concepts compared to the full area Al-BSF (see Fig. 9).

The reflection graphs are displayed in Fig. 10. The better rear surface reflectivity of evaporated aluminum compared to screen printed aluminum is clearly visible at 1100 nm.

Due to the better rear surface reflectivity of the evaporated aluminum the LFC cells have a higher IQE in the range of 1000 to 1200 nm wavelength. Below 1000 nm the SP-LBSF cells show a better IQE because the BSF has a higher passivation quality.
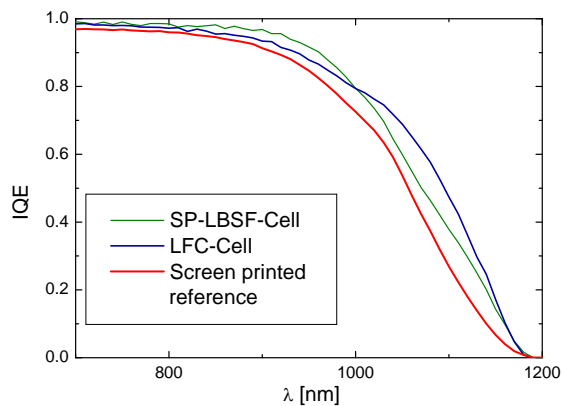
Figure 9: IQE of solar cells with LFC, SP-LBSF and full area Al-BSF rear side contacting. The solar cell with full area Al-BSF was processed in a different batch as the other two solar cells.
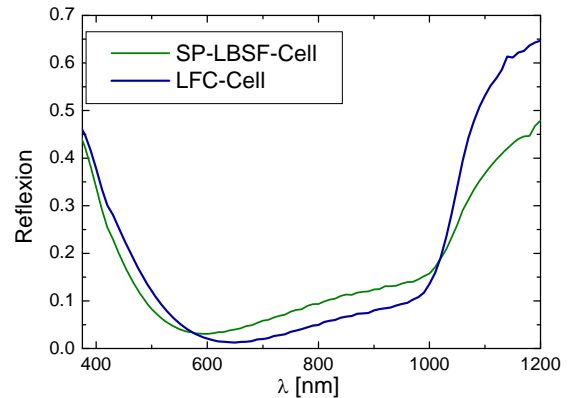
Figure 10: Reflection graphs of solar cells with LFC and SP-LBSF rear side contacting without texture.

7   CONCLUSION AND OUTLOOK

Manufacturing processes for the investigated local rear side structures were developed. Both local rear contact concepts showed a better performance in the IQE at long wavelengths compared to the full area Al-BSF structure. The LFC concept had an improved rear side reflection due to the evaporated aluminum. Further changes in the order of the processing steps could possibly enhance the LFC cells. For the solar cells with local screen printed BSF, an optimization of the contact design could further improve the performance.

8   ACKOWLEDGEMENTS

9   REFERENCES

[1] M. Hermle et al., Proc. 20th EUPVSEC, Barcelona, 2005, 810
[2] E. Schneiderlöchner et al., Proc. 19th EUPVSEC, Paris, 2004, 447
[3] R. Pavlović, Diploma thesis, Konstanz, 2009
[4] S.W. Glunz et al., Proc. 20th EUPVSEC, Barcelona, 2005, 572